

Cytochrome *b* Mutations That Modify the Ubiquinol-binding Pocket of the Cytochrome *bc*₁ Complex and Confer Anti-malarial Drug Resistance in *Saccharomyces cerevisiae**

Received for publication, January 11, 2005, and in revised form, February 4, 2005
Published, JBC Papers in Press, February 17, 2005, DOI 10.1074/jbc.M500388200

Jacques J. Kessler[‡], Kevin H. Ha[‡], Anne K. Merritt[‡], Benjamin B. Lange[‡], Philip Hill[§],
Brigitte Meunier[§], Steven R. Meshnick[¶], and Bernard L. Trumpower[‡]||

From the [‡]Department of Biochemistry, Dartmouth Medical School, Hanover, New Hampshire 03755, [§]Wolfson Institute for Biomedical Research, University College London, London WC1E6BT, United Kingdom, and [¶]Department of Microbiology and Immunology, University of North Carolina, Chapel Hill, North Carolina 27599

Atovaquone is a new anti-malarial agent that specifically targets the cytochrome *bc*₁ complex and inhibits parasite respiration. A growing number of failures of this drug in the treatment of malaria have been genetically linked to point mutations in the mitochondrial cytochrome *b* gene. To better understand the molecular basis of atovaquone resistance in malaria, we introduced five of these mutations, including the most prevalent variant found in *Plasmodium falciparum* (Y268S), into the cytochrome *b* gene of the budding yeast *Saccharomyces cerevisiae* and thus obtained cytochrome *bc*₁ complexes resistant to inhibition by atovaquone. By modeling the variations in cytochrome *b* structure and atovaquone binding with the mutated *bc*₁ complexes, we obtained the first quantitative explanation for the molecular basis of atovaquone resistance in malaria parasites.

Up to one-half billion people in the world suffer from malaria with various degrees of severity. The disease kills more than 2.7 million people a year, most of them children under 5 years old in sub-Saharan Africa (1). Over the past three decades, the parasite that causes malaria, *Plasmodium falciparum*, has developed resistance to almost every commonly available anti-malarial drug, including chloroquine, pyrimethamine, cycloguanil, and sulfadoxine. Because some of these drugs are now almost useless in many parts of the world, the rapid spread of resistant parasites is a serious global health problem in endemic countries.

In the 1990s, the urgent need for new anti-malarial drugs for treatment and chemoprophylaxis led to the development of atovaquone (2-[*trans*-4-(4'-chlorophenyl)cyclohexyl]-3-hydroxy-1,4-hydroxynaphthoquinone). This recently introduced anti-malarial compound, which has broad spectrum activity against apicomplexan parasites (2–4), also prevents and clears *Pneumocystis pneumonia* (5). Atovaquone is a potent and specific inhibitor of the cytochrome *bc*₁ complex (EC 1.10.2.2) (6), an essential respiratory enzyme present in the inner mitochondrial membrane. This drug was approved by the FDA in 1995 and is now distributed as a synergic combination with proguanil hydrochloride under the trade name of Malarone®. Despite minimal side effects and high activity against malaria, the cost

of Malarone® treatment has, until now, restricted its use to western non-immune adult and children (7) travelers and some European military personnel (8).

Unfortunately, there is growing evidence that malarial parasites may quickly develop drug resistance by mutation of amino acid residues located in or near the atovaquone-binding site on cytochrome *b* (9–11). Within just a few years after its introduction, the mitochondrial DNA sequences of isolates of *P. falciparum* associated with Malarone® treatment failures exhibit the same Y268S (malaria numbering) mutation of the cytochrome *b* gene of the parasite. Because these isolates were obtained from infected patients returning from Thailand (12), Ivory Coast (13), Mali (14), Cameroon (15), and Kenya (16), growing concern about the spread and the high frequency of this mutation led to the design of PCR-based screening procedures in Europe for quick detection in case of Malarone® treatment failure (14, 17, 18).

Because the yeast *bc*₁ complex is also inhibited by atovaquone (6), we previously developed *Saccharomyces cerevisiae* as a model to study cytochrome *b* mutations conferring atovaquone resistance in *Pneumocystis* (19, 20). In the present study we transferred several mutations associated with atovaquone resistance in *Plasmodium yoelii* (9) and *P. falciparum* (10, 12–16) into the yeast cytochrome *b* gene. This allowed us to biochemically confirm the linkage of atovaquone resistance to the cytochrome *b* mutations and to explain at the molecular level the mechanism by which malaria parasites counter the therapeutic cytotoxicity of this new drug.

EXPERIMENTAL PROCEDURES

Materials—Yeast extract and peptone were from Difco. Nitrogen base without amino acids but with ammonium sulfate was from U. S. Biological. Dodecylmaltoside was obtained from Roche Applied Science. DEAE-Biogel A was obtained from Bio-Rad. Decyl ubiquinone, diisopropylfluorophosphate, and dithionite were purchased from Sigma. Stigmatellin was purchased from Fluka Biochemica. Atovaquone was a gift from GlaxoSmithKline.

Purification of Cytochrome *bc*₁ Complexes—The cytochrome *b* mutations were introduced into the mitochondrial cytochrome *b* gene by biolistic transformation as described elsewhere (19). Wild-type and mutated yeast strains were grown in yeast extract/peptone/dextrose medium and harvested by centrifugation. Cytochrome *bc*₁ complexes were then isolated from mitochondria as described previously (21, 22).

Measurement of Oxygen Consumption and Ubiquinol-Cytochrome *c* Reductase Activity—Rates of oxygen uptake by intact yeast cells were measured at 25 °C with a Gilson oxygraph and a polarographic oxygen electrode (Gilson Medical Electronics, Middleton, WI) as described previously (23). Cytochrome *c* reductase activities of the cytochrome *bc*₁ complexes were assayed in 50 mM potassium phosphate, pH 7.0, 250 mM sucrose, 0.2 mM EDTA, 1 mM Na₂S₂O₃, 2.5 mM KCN, 0.01% Tween 20, and 40 μM cytochrome *c* at 23 °C. The cytochrome *bc*₁ complex was diluted to 2.5 nM in the assay buffer, and the reaction was started by adding

* The costs of publication of this article were defrayed in part by the payment of page charges. This article must therefore be hereby marked "advertisement" in accordance with 18 U.S.C. Section 1734 solely to indicate this fact.

|| To whom correspondence should be addressed: Dept. of Biochemistry, Dartmouth Medical School, 7200 Vail, Hanover, NH 03755. Tel.: 603-650-1621; E-mail: Trumpower@Dartmouth.edu.

2,3-dimethoxy-5-methyl 6-decyl-1,4-benzoquinol, an analogue of ubiquinol. The reduction of cytochrome *c* was monitored in an Aminco DW-2a spectrophotometer at 550 versus 539 nm in dual wavelength mode. Data were collected and analyzed using an Online Instrument Systems Inc. computer interface and software.

Molecular Modeling—Molecular modeling was carried out on a Silicon Graphics O2 work station using the commercially available Insight II® software package (Accelrys Inc., San Diego, CA). The starting structure was the energy-minimized atovaquone-bound yeast cytochrome *bc*₁ complex (6). Each cytochrome *b* mutation, Y279S, Y279C, I269M, L282V, and F278I, was built separately into the atovaquone-bound center P site using the lowest energy manual rotamer selected by the Biopolymer® module.

For each structure, a flexible subset of adjacent residues within 2.0 Å of the mutation was selected. A surrounding 9.5-Å shell of residues, including atovaquone, was kept fixed. Residues beyond this shell were excluded from calculations in the interest of speed. The atom-based cut-off for non-bonding interactions was set at 9.5 Å, and the dielectric constant was set at 2.0. The CFF91 force field, which uses a 6–9 Lennard-Jones potential to calculate van der Waals interactions, was used for all modeling.

A five-step simulated annealing run, from 800 to 298 K, was performed on each mutated structure using the Discover 3® module in Insight II®. At each of the five temperatures, the Nosé temperature control method was used for a simulation time of 10,000 fs/step, with a 0.5 fs/iteration time step. The final structure was minimized to a final convergence of 0.001 using Cauchy's steepest descent, conjugate gradient, and Newton methods consecutively. Five simulated annealing runs were carried out for each mutant structure to obtain an average final energy.

To estimate the energy cost of binding atovaquone, we calculated the energy of each mutant structure with the bound atovaquone and compared it with the energy of the wild-type enzyme with bound atovaquone. To compare non-bonding interaction energies (van der Waals and electrostatic) and internal conformation energies of mutant and wild-type structures, a common subset (20), including atovaquone, the residue His-181 on the iron-sulfur protein, cytochrome *b* residues within 4.0 Å of the inhibitor, and cytochrome *b* residues within 4.0 Å of cytochrome *b* residue Glu-272, was used for all calculations.

RESULTS

Location of the Cytochrome *b* Mutations Conferring Atovaquone Resistance to *Plasmodium*—The molecular target of atovaquone is now known to be the ubiquinol oxidation pocket at the center P site of the cytochrome *bc*₁ complex (6). An energy-minimized structure of atovaquone in the ubiquinol oxidation pocket obtained by molecular modeling indicated that the hydroxyl group of the hydroxy-naphthoquinone bound via a hydrogen bond to the nitrogen of His-181 of the Rieske iron-sulfur protein. This hydrogen bonding accounts for the effects of atovaquone on the midpoint potential of the Rieske protein (6) and mimics the hydrogen bond between undecyl hydroxy benzoxythiazol and the Rieske protein in the crystal structure of the undecyl hydroxy benzoxythiazol-bound *bc*₁ complex (24). On the opposite side of the ring system, the carbonyl group at position 4 of the quinone ring of atovaquone formed a water-mediated hydrogen bond with Glu-272 of cytochrome *b*. The remainder of the molecular interactions between atovaquone and cytochrome *b* were essentially hydrophobic with a network of aromatic and aliphatic side chains surrounding the inhibitor. This binding pattern is similar to the one recently found in the crystal structure of the yeast *bc*₁ complex with undecyl hydroxy benzoxythiazol, a hydroxyquinone, bound to the ubiquinol oxidation pocket (24).

Because there is a high degree of sequence identity (about 68%) between *S. cerevisiae* and *Plasmodium* cytochrome *b* within the atovaquone-binding pocket (Fig. 1), we chose the yeast for studying how mutations can affect the drug efficacy. All atovaquone-resistant mutations in the cytochrome *b* sequence found in *Plasmodium* were localized around this binding site (9–14, 25). Five of these mutations associated with resistance in *P. yoelii* (9) and *P. falciparum* (10–16) (Fig. 1)

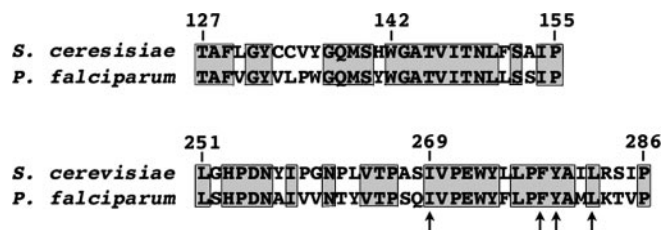


FIG. 1. Sequence alignment of the cytochrome *b* proteins of *S. cerevisiae* and *P. falciparum* in the conserved regions including residues 127–155 and 251–286 around the ubiquinol oxidation pocket at the center P site. The alignment was constructed using ClustalW and yeast numbering. The arrows show the positions of the mutated residues in *Plasmodium*.

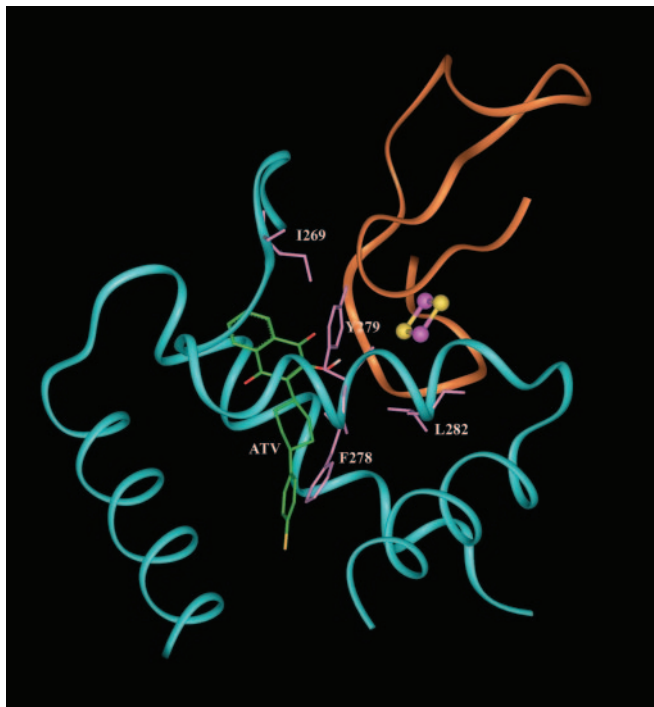


FIG. 2. View of the atovaquone-binding pocket of the yeast cytochrome *bc*₁ complex showing the location of mutations conferring resistance to atovaquone in *Plasmodium*. Cytochrome *b* is shown in cyan, and a portion of the Rieske iron-sulfur protein is in gold. The iron-sulfur cluster is at the top right, with iron and sulfur atoms colored purple and yellow, respectively. The carbon atoms in atovaquone (ATV) are green, oxygen atoms are red, and hydrogen atoms are white. The mutated residues are purple.

were transferred into the *S. cerevisiae* cytochrome *b* gene by the biolistic method (19).

The modeled structure of the yeast ubiquinol oxidation pocket at the center P site with bound atovaquone and the location of the amino acids residues affected in the atovaquone-resistant cytochrome *b* mutants are shown in Fig. 2. These five mutations are I258M, F267I, Y268C, Y268S, and L271V in *Plasmodium* numbering, equivalent to I269M, F278I, Y279C, Y279S, and L282V in the yeast numbering system (we will use *S. cerevisiae* numbering of cytochrome *b* hereafter). Except for I269M, which is located in the EF loop, all of the mutations affect residues of the EF helix of cytochrome *b*.

Loss of Fitness Associated with the Cytochrome *b* Mutations—Growth of the five mutated strains was monitored in a non-fermentable medium to study the impact of the mutations on the respiration of the yeast cells. The growth curves (Fig. 3A) reveal that, in contrast to a doubling time of 6 (\pm 0.5) h observed for the wild-type strain and also for the I269M and F278I mutants, the Y279C mutated strain had a doubling time

FIG. 3. Fitness of mutated yeast strains. *A*, growth curves of wild-type and mutated *S. cerevisiae* strains in non-fermentable medium. Culture densities are expressed in optical density at 600 nm (*OD*₆₀₀). The strains are wild type (◆), F278I (●), I269M (▲), Y279C (■), Y279S (□), and L282V (+) mutants. *B*, rates of oxygen consumption by wild-type (WT) and mutant *S. cerevisiae* strains. Oxygen uptake rates are expressed in nanoatoms of oxygen/10⁷ yeast cells/min.

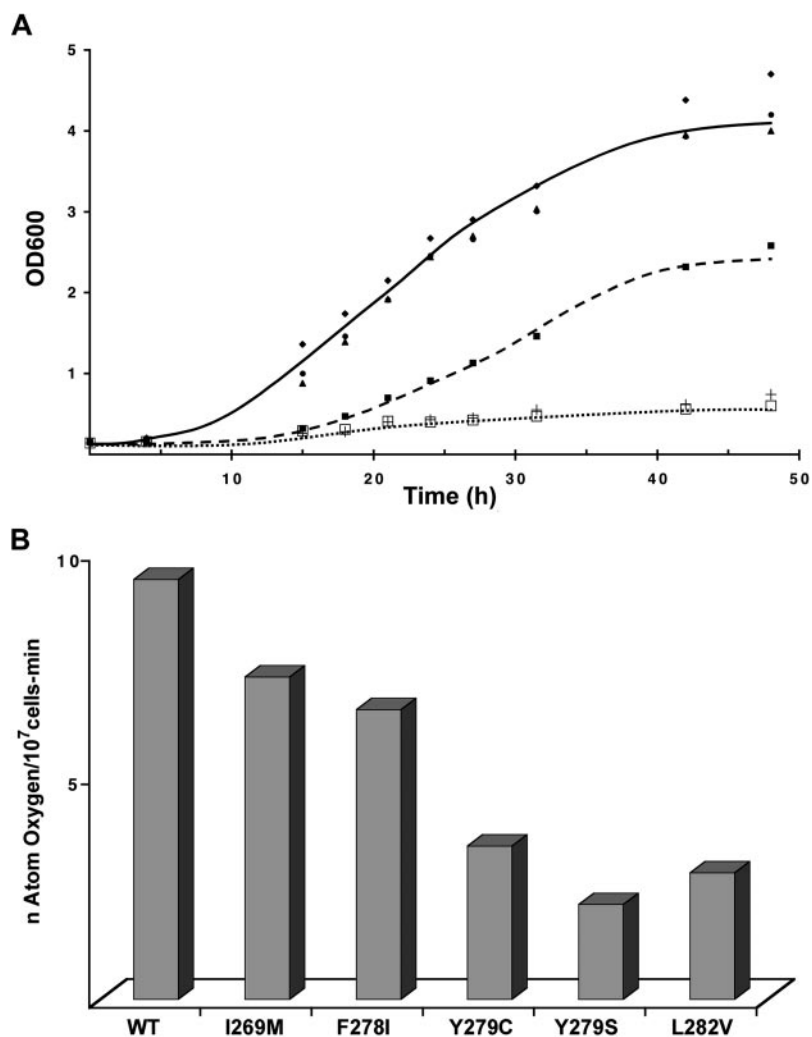


TABLE I
Kinetic parameters of purified cytochrome *bc₁* complexes from wild-type and atovaquone-resistant yeast mutants

Yeast strains	k_{cat} s^{-1}	K_M μM
Wild type	220	13
I269M	30	8
F278I	220	13
Y279C	10	ND ^a
Y279S	20	ND
L282V	15	ND

^a ND, not determined.

of 9 (\pm 0.5) h. In addition, both the Y279S and L282V mutants show even more severe growth defects, with doubling times of 13 (\pm 0.5) h.

Measurements of oxygen consumption of the yeast cells in mid-log growth phase (Fig. 3B) confirmed a decrease of >60% of the respiratory function for the Y279C, Y279S, and L282V mutated strains. To further investigate this effect, the cytochrome *bc₁* complex was purified from the mitochondria of each strain to assess the kinetic parameters of the enzymes (Table I). Again, the *bc₁* complexes from the three mutants Y279C, Y279S, and L282V that showed significant defects in growth rates and oxygen consumption also showed activity losses of >90% compared with the wild-type strain. These activities were too low to permit accurate determination of K_m and V_m

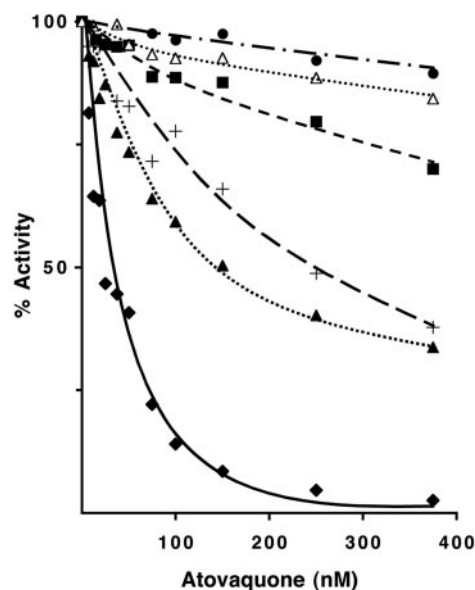


FIG. 4. Relative efficacy of inhibition of wild-type and mutated *bc₁* complexes by atovaquone. Ubiquinol-cytochrome *c* reductase activities of purified *bc₁* complexes were measured in the presence of increasing concentrations of atovaquone. Activities are expressed as a percentage of the activity of each *bc₁* complex in the absence of inhibitor and are indicated as follows: ◆, wild-type; ■, Y279C; □, Y279S; ▲, I269M; +, F278I; and ●, L282V.

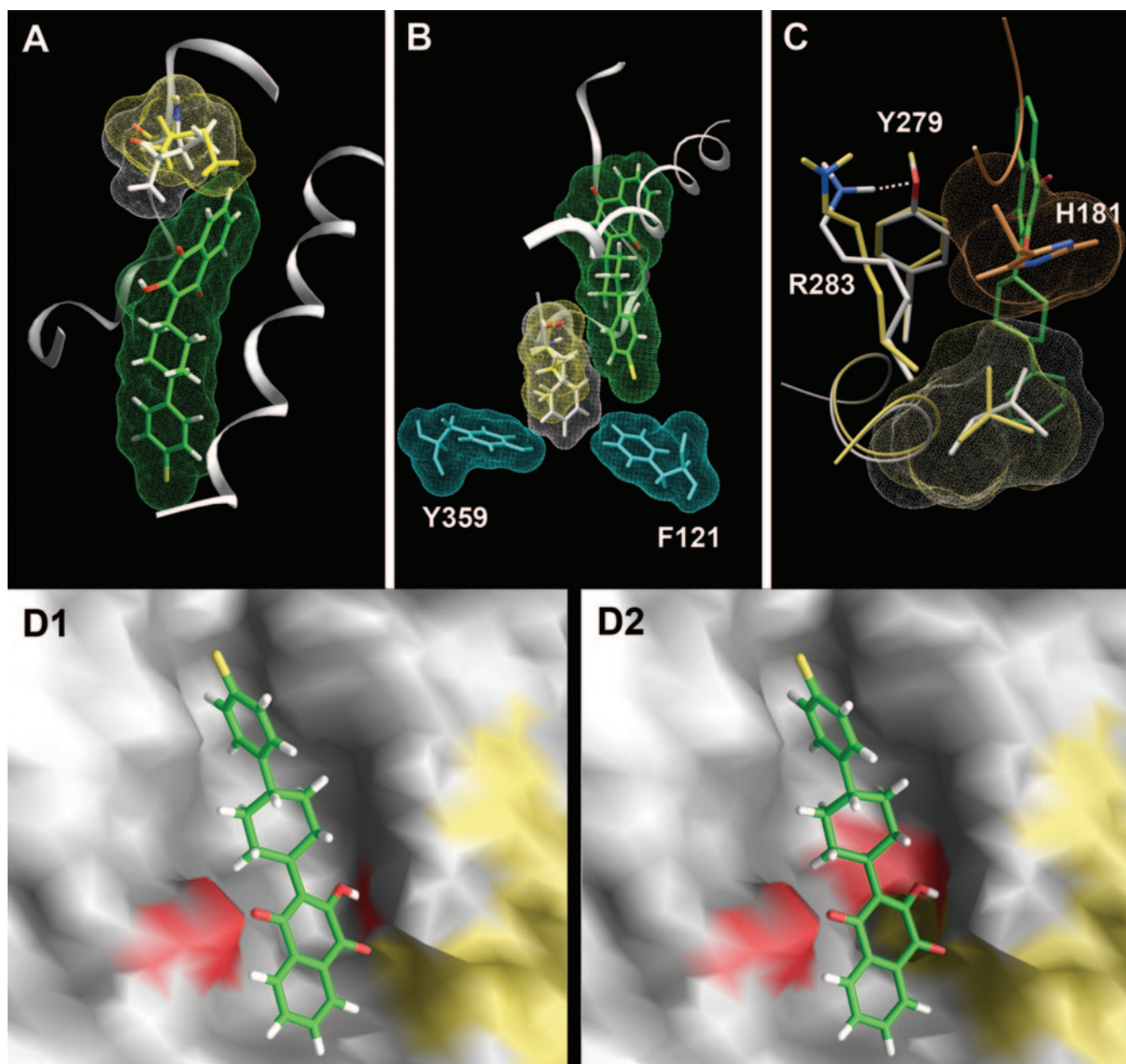


FIG. 5. **Molecular modeling of atovaquone-resistant mutations of the bc_1 complex from *Plasmodium* in *S. cerevisiae*.** A–C, mutations I269M, F278I, and L282V. For clarity, only atovaquone (green), wild-type residues (white), mutated residues (yellow), important aromatic interacting residues (cyan), His-181 from the iron-sulfur protein (orange), and the affected residues Tyr-279 and Arg-283 are shown. D, views of atovaquone binding in the bc_1 complexes of wild-type yeast (D1) and the Y279S or Y279C mutants (D2). The figure was generated using GRASP software. The chlorine on atovaquone is yellow, oxygens are red, and hydrogens are white. The yellow surface corresponds to the Rieske iron-sulfur protein. The white surfaces were generated by hydrophobic and aromatic residues of the cytochrome *b*, and the red surfaces were generated by hydrophilic and nucleophilic side chains.

values. The activity of the bc_1 complex from the I269M mutant was also low, although the growth rates and rates of oxygen consumption by this yeast mutant were similar to and only slightly less than those of the wild-type strain. This suggested that the bc_1 complex from the I269M mutant suffered some loss of activity during isolation.

Western blots indicated no loss of iron-sulfur protein, and optical spectra indicated no assembly defects in cytochromes *b* or *c*₁ that could account for these decreases of respiratory function. Thus the results clearly suggest that these three cytochrome *b* mutations associated with atovaquone resistance in *Plasmodium* impair the ubiquinol-binding properties of the yeast bc_1 complex. Possible implications of this effect for the growth of the parasite are discussed below.

Effect of Cytochrome b Mutations on Inhibition of the bc_1 Cytochrome Complex by Atovaquone—Ubiquinol-cytochrome *c* reductase activities of the purified bc_1 complexes from the wild-type and mutated yeast strains were measured in the presence of increasing concentrations of atovaquone to test whether sensitivity of the enzymes to the drug was altered by the cytochrome *b* mutations. We have shown previously that the bc_1 complex of wild-type yeast is sensitive to atovaquone with an inhibitor concentration of ~25 nM required for 50% inhibition of the activity of the purified enzyme (6). As shown in Fig. 4, all of the cytochrome *b* mutations that confer atovaquone resistance to the *Plasmodium* also altered the IC₅₀ for inhibition of the yeast bc_1 complex and by various amounts. The I269M and F278I mutations had the smallest effect, but

even these conferred a 5–10-fold increase in resistance, with IC_{50} values between 150–250 nM. The Y279C, Y279S, and L282V were the three cytochrome *b* mutations showing the highest level of resistance to the atovaquone, with IC_{50} values between 1 and 2 μ M. This corresponded to a 40–80-fold increase over the concentration required to inhibit the wild-type enzyme.

Structural Changes in Cytochrome *b* Caused by Mutations Conferring Resistance to Atovaquone—The five cytochrome *b* mutations responsible for atovaquone resistance in *Plasmodium* were built into the previously modeled atovaquone-bound ubiquinol oxidation pocket at the center P site of the yeast *bc*₁ complex (6), and the structural changes resulting from the mutations were modeled *in silico*. The isoleucine at position 269, located in a hydrophobic region of the binding pocket, interacted directly with the naphthoquinone ring of atovaquone. Modeling of the I269M mutation (Fig. 5A) showed a decrease of the volume available in this hydrophobic pocket, which interfered with binding of the inhibitor.

The phenylalanine at position 278 interacted directly with the chlorophenyl substituent of atovaquone. Examination of this region revealed the presence of an aromatic cluster composed of Phe-121, Phe-278, Tyr-359 and the chlorophenyl group of the atovaquone (Fig. 5B). The F278I mutation removed the central aromatic element of this cluster, destabilized this area of the pocket, and thus interfered with binding of the drug.

Tyrosine 279 is also contained in a stable aromatic cluster composed of His-181 of the Rieske protein and the naphthoquinone group of the ligand. The modeling results in Fig. 5D clearly show how the Y279C or Y279S mutations, which replace an aromatic group by strong nucleophilic side chains, decreased the hydrophobic interactions between the binding pocket and the atovaquone.

In the L282V mutant, two changes taking place simultaneously explain the decrease of atovaquone binding as shown in Fig. 5C. First, Leu-282 interacted slightly with His-181 of the Rieske protein subunit, and the L282V mutation modified this interaction and influenced the degree of freedom of His-181. Secondly, the reduction in size of the aliphatic side chain created an empty space that the modeling compensated for by adjusting the backbone geometry of residues 280–285. Examination of this region showed that this adjustment suppressed a hydrogen bond between Arg-283 and Tyr-279 (Fig. 5C), which caused a change in the orientation of Tyr-279 toward the binding pocket. Consequently, displacement of the Tyr-279 residue caused an atovaquone-binding defect similar to the ones observed for the Tyr-279 mutants and contributed to the effect of the His-181 positioning.

Calculation of Changes in Atovaquone-binding Energy Resulting from Mutations in Cytochrome *b*—The energy required for binding atovaquone was calculated with each of the modeled structures. The calculated changes in binding energy were then compared with the experimentally measured changes in IC_{50} values. The changes in atovaquone-binding energy with the *bc*₁ complexes from the mutants relative to the binding energy obtained for the wild-type enzyme and the changes in IC_{50} values for the mutant enzymes compared with the wild-type enzyme are shown in Fig. 6. The relative increase in calculated binding energy correlated well with the relative increase in IC_{50} values for the *bc*₁ complexes for each mutation, with the exception of L282V. This mutation, which displayed the largest change among the IC_{50} values, did not yield a comparably large increase in calculated binding energy. Possible reasons for this difference are discussed below.

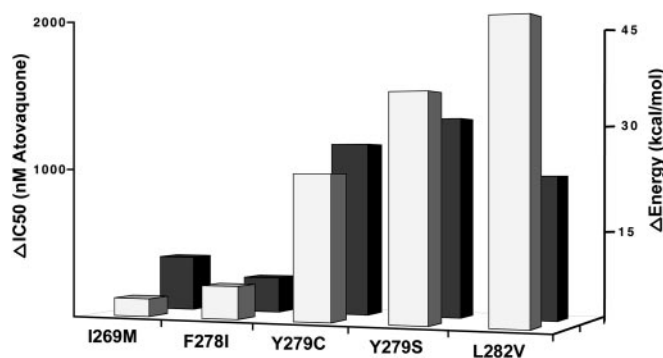


FIG. 6. Measured changes in atovaquone inhibition and modeled changes in atovaquone binding with atovaquone-resistant cytochrome *bc*₁ complexes. The light gray bars indicate the change in IC_{50} for inhibition of the *bc*₁ complexes by atovaquone compared with inhibition of the enzyme from wild-type yeast. The dark bars show the calculated change in binding energy for atovaquone with each of the mutated *bc*₁ complexes versus that with the wild-type enzyme.

DISCUSSION

Only a decade after the introduction of the anti-malarial drug atovaquone, new strains of *P. falciparum* that are resistant to the therapy have emerged worldwide. In this work, we used the budding yeast *S. cerevisiae* as a surrogate to recapitulate and understand the molecular basis of the atovaquone resistance found in the malaria parasites. It is well known that atovaquone suppresses the respiratory function of the parasite by inhibiting the cytochrome *bc*₁ complex (26). The drug is also a potent inhibitor of the yeast *bc*₁ complex (6), and the binding sites of the enzyme in the two microorganisms show a high degree of identity.

We have previously elucidated the mechanism of atovaquone inhibition of the *bc*₁ complex and developed a molecular model of atovaquone interaction with the ubiquinol oxidation pocket of the enzyme that accounts for the effects of the drug on the isolated enzyme (6). The strong and highly specific binding between the *bc*₁ complex and atovaquone results from a combination of aromatic interactions and several hydrogen bonds, some of which mimic the binding determinants of the natural substrate, ubiquinol. Atovaquone is thus a competitive inhibitor of the enzyme.

Most of the atovaquone-resistant malaria strains contain point mutations in the mitochondria-encoded cytochrome *b* gene. We were able to transfer these mutations into the yeast mitochondrial genome using a biolistic transformation procedure. Some of the resulting mutants were unable to grow on non-fermentable carbon sources, and thus it was not possible to demonstrate atovaquone resistance *in vivo*. However, the *bc*₁ complexes purified from the mutated strains exhibited large decreases in sensitivity toward atovaquone. We were thus able to biochemically confer the genetic evidence that linked these mutations to atovaquone resistance.

A previous study done on *Plasmodium* (9) demonstrates that these mutations can be ranked by the effects of atovaquone on the collapse of the mitochondrial membrane potential of the parasite. This ranking resulted in moderate atovaquone resistance for I269M and F278I and greater resistance for Y279C and L282V. Notably, these mutations transferred into *S. cerevisiae* produced the same ranking order, demonstrating that the yeast *bc*₁ complex is a valuable model for atovaquone resistance.

In a recent study of mutations conferring atovaquone resistance in pathogenic *Pneumocystis* fungi, we show that one-half of the mutations are distal from the drug-binding pocket, and these are able to remotely modify the drug-binding properties of the *bc*₁ complex (20). Interestingly, all of the *Plasmodium*

mutations that we duplicated in yeast in the present study affected residues located in the binding pocket and interacting directly with the atovaquone. The molecular modeling simulations were able to describe the effects of each point mutation on the geometry of the atovaquone-binding pocket at the molecular level.

The molecular modeling revealed that the I269M mutation, which includes the insertion of a bulkier residue, is a typical example of resistance acquired by increasing steric constraints on the inhibitor. Several atovaquone-resistant mutations (I147V, L150F, and L275F) found in *Pneumocystis* have been shown to have analogous steric effects (20).

The three mutations F278I, Y279S, and Y279C removed an aromatic residue localized near the atovaquone and suppressed important interactions between the drug and the binding pocket. Likewise, molecular modeling of the L282V mutation showed that the mutation caused the rotation of Tyr-279 and, consequently, a variation of aromatic interaction with the atovaquone. Tight binding to the same locus using a very similar aromatic network has been described for the fungicide famoxadone, another inhibitor of the *bc*₁ complex (27). Interestingly, *Plasmodium*, *Saccharomyces*, and *Pneumocystis*, which have atovaquone-sensitive *bc*₁ complexes, all have a phenylalanine in position 278 of cytochrome *b*, whereas the bovine and human cytochrome *bc*₁ complexes, which are relatively insensitive to atovaquone, have an alanine at the equivalent cytochrome *b* position. The 278 locus thus appears to be important for the differential efficacy of the drug, similar to the position 275 (6).

The importance of Tyr-279 in cytochrome *b* for *bc*₁ activity is supported by its conservation among species. It has been postulated that the aromatic side chain of this tyrosine participates in the positioning of ubiquinol, the natural substrate of the enzyme (24). In *Rhodobacter sphaeroides* (28), mutation of the homologous tyrosine has no effect on the activity when replaced by phenylalanine, a small effect (3-fold decrease) when replaced by leucine, and a dramatic effect (20-fold decrease) when replaced with a glycine. In yeast (29), mutation of the same tyrosine into alanine causes an ~5-fold decrease in *bc*₁ complex activity. Therefore, the 279 position appears to require an aromatic side chain, or at least a large hydrophobic residue, to maintain a functional *bc*₁ complex. Furthermore, when this position is occupied by a nucleophilic residue such as cysteine (Y279C) or serine (Y279S), the activity is severely compromised. The sulfur atom of the cysteine being less electronegative than the oxygen atom of the serine would account for the differences between the two mutations. The Y279C mutation has also been observed clinically in a human *bc*₁ complex, in which case the mutation was associated with severe exercise intolerance, deafness, and mental retardation (29, 30).

The comparison of experimentally measured changes in IC₅₀ values for inhibition by atovaquone and theoretically calculated changes in binding energies provides a useful check on the validity of the molecular modeling. With one exception, there was generally good agreement between these two parameters. The one outlier, the L282V mutation, exhibited a relatively greater change in IC₅₀ than would be predicted from the calculated change in binding energy. This may reflect the fact that IC₅₀ is a free energy (ΔG) term, which includes an entropic parameter, whereas the calculated binding energy is solely enthalpic (ΔH). Alternatively, the divergence for this mutation may be because of a failure of the molecular mechanics algorithms to accurately evaluate the energy variation associated with the rotation of an element of a stable aromatic cluster.

It is extremely challenging and costly to establish malaria

cultures from patient blood (and probably impossible to do so in third world country facilities), so it is difficult to prove that a specific novel mutation of the cytochrome *b* gene is responsible for a specific patient failing treatment with Malarone®. The yeast model makes it possible to demonstrate and quantify which mutations confer atovaquone resistance and which are just coincidental allele variations.

Two of the mutations, Y279S and L282V, severely impaired the ability of the yeast strains to grow on a non-fermentable carbon source. It has been observed that some atovaquone-resistant mutations cause changes in cytochrome *b*, leading to a loss of fitness in the malaria parasite (31). This is frequently observed in mutations that confer drug resistance to microorganisms by alteration of structurally important regions of the target molecules (32, 33). In the case of atovaquone, this loss of fitness results from mutations close to the active site that reduce the binding of the ubiquinol substrate by the enzyme. There is no report that the widespread Y279S mutation causes a loss of fitness in *P. falciparum*, but our yeast model strongly predicts it. The implication of this prediction is important for the future development and use of the drug Malarone®, because it suggests that the geographic spreading of a single locus change such as the Y279S mutation will be stopped by the removal of the drug. As the resistant strain has to compete against a more fit, wild-type parasite, the reversal of atovaquone resistance will happen spontaneously.

REFERENCES

- Breman, J. G. (2001) *Am. J. Trop. Med. Hyg.* **64**, 1–11
- Fry, M., and Pudney, M. (1992) *Biochem. Pharmacol.* **43**, 1545–1553
- Araujo, F. G., Huskinson, J., and Remington, J. S. (1991) *Antimicrob. Agents Chemother.* **35**, 293–299
- Hughes, W. T., and Oz, H. S. (1995) *J. Infect. Dis.* **172**, 1042–1046
- Hughes, W. T., Gray, V. L., Gutteridge, W. E., Latter, V. S., and Pudney, M. (1990) *Antimicrob. Agents Chemother.* **34**, 225–228
- Kessl, J. J., Lange, B. B., Merbitz-Zahradnick, T., Zwicker, K., Hill, P., Meunier, B., Palsdottir, H., Hunte, C., Meshnick, S., and Trumppower, B. L. (2003) *J. Biol. Chem.* **278**, 31312–31318
- Camus, D., Djossou, F., Schilthuis, H. J., Hogh, B., Dutoit, E., Malvy, D., Roskell, N. S., Hedgley, C., De Boever, E. H., and Miller, G. B. (2004) *Clin. Infect. Dis.* **38**, 1716–1723
- Petersen, E. (2003) *J. Travel Med.* **10**, S13–S15
- Srivastava, I. K., Morrissey, J. M., Darrouzet, E., Daldal, F., and Vaidya, A. B. (1999) *Mol. Microbiol.* **33**, 704–711
- Suswam, E., Kyle, D., and Lang-Unnasch, N. (2001) *Exp. Parasitol.* **98**, 180–187
- Fivelman, Q. L., Butcher, G. A., Adagu, I. S., Warhurst, D. C., and Pasvol, G. (2002) *Malar. J.* **1**, 1
- Korsinczyk, M., Chen, N., Kotecka, B., Saul, A., Rieckmann, K., and Cheng, Q. (2000) *Antimicrob. Agents Chemother.* **44**, 2100–2108
- Farnert, A., Lindberg, J., Gil, P., Swedberg, G., Berqvist, Y., Thapar, M. M., Lindegardh, N., Berezcky, S., and Bjorkman, A. (2003) *Br. Med. J.* **326**, 628–629
- Schwobel, B., Alifrangis, M., Salanti, A., and Jelinek, T. (2003) *Malar. J.* **2**, 5
- David, K. P., Alifrangis, M., Salanti, A., Vestergaard, L. S., Ronn, A., and Bygberg, I. (2003) *Scand. J. Infect. Dis.* **35**, 897–898
- Schwartz, E., Bujanover, S., and Kain, K. C. (2003) *Clin. Infect. Dis.* **37**, 450–451
- Gil, J. P., Nogueira, F., Stromberg-Norklit, J., Lindberg, J., Carrolo, M., Casimiro, C., Lopes, D., Ares, A. P., Cravo, P. V., and Rosario, V. E. (2003) *Mol. Cell. Probes* **17**, 85–89
- Wichmann, O., Muehlberger, N., Jelinek, T., Alifrangis, M., Peyerl-Hoffmann, G., Muhlen, M., Grobusch, M. P., Gascon, J., Matteelli, A., Laferl, H., Bisoffi, Z., Ehrhardt, S., Cuadros, J., Hatz, C., Gjørup, I., McWhinney, P., Beran, J., da Cunha, S., Schulze, M., Kollaritsch, H., Kern, P., Fry, G., and Richter, J. (2004) *J. Infect. Dis.* **190**, 1541–1546
- Hill, P., Kessl, J., Fisher, N., Meshnick, S., Trumppower, B. L., and Meunier, B. (2003) *Antimicrob. Agents Chemother.* **47**, 2725–2731
- Kessl, J. J., Hill, P., Lange, B. B., Meshnick, S. R., Meunier, B., and Trumppower, B. L. (2004) *J. Biol. Chem.* **279**, 2817–2824
- Snyder, C. H., and Trumppower, B. L. (1999) *J. Biol. Chem.* **274**, 31209–31216
- Ljungdahl, P. O., Pennoyer, J. D., Robertson, D., and Trumppower, B. L. (1987) *Biochim. Biophys. Acta* **891**, 227–242
- Atlante, A., Calissano, P., Bobba, A., Azzariti, A., Marra, E., and Passarella, S. (2000) *J. Biol. Chem.* **275**, 37159–37166
- Palsdottir, H., Lojero, C. G., Trumppower, B. L., and Hunte, C., (2003) *J. Biol. Chem.* **278**, 31303–31311
- Syafuruddin, D., Siregar, J. E., and Marzuki, S. (1999) *Mol. Biochem. Parasitol.* **104**, 185–194
- Hudson, A. T. (1993) *Parasitol. Today* **9**, 66–68
- Gao, X., Wen, X., Yu, C. A., Esser, L., Tsao, S., Quinn, B., Zhang, L., Yu, L., and Xia, D. (2002) *Biochemistry* **41**, 11692–11702
- Crofts, A. R., Guergova, K., Kuras, R., Ugulava, N., Li, J., and Hong, S. (2000)

- Biochim. Biophys. Acta* **1459**, 456–466
29. Fisher, N., Castleden, K., Bourges, I., Brasseur, G., Dujardin, G., and Meunier, B. (2004) *J. Biol. Chem.* **279**, 12951–12958
30. Wibrand, F., Ravn, K., Schwartz, M., Rosenberg, T., Horn, N., and Vissing, J. (2001) *Ann. Neurol.* **50**, 540–543
31. Peters, J. M., Chen, N., Gatton, M., Korsinczky, M., Fowler, E. V., Manzetti, S., Saul, A., and Cheng, Q. (2002) *Antimicrob. Agents Chemother.* **46**, 2435–2441
32. Billington, O. J., McHugh, T. D., and Gillespie, S. H. (1999) *Antimicrob. Agents Chemother.* **43**, 1866–1869
33. Devereux, H. L., Emery, H. L., Johnson, M. A., and Loveday, C. (2001) *J. Med. Virol.* **65**, 218–224